KSÜ Tarım ve Doğa Derg 25 (Ek Sayı 1): 72-84, 2022
KSU J. Agric Nat 25 (Suppl 1): 72-84, 2022
https://doi.org/10.18016/ksutarimdoga.vi.1036488

Rapid Biosynthesis of Silver Nanoparticles by *Celtis tournefortii* LAM. Leaf Extract; Investigation of Antimicrobial and Anticancer Activities

Ayşe BARAN[1], Cumali KESKIN[2]✉, Sevgi İrtegün KANDEMIR[3]
[1]Department of Biology, Graduate Education Institute, Mardin Artuklu University, Mardin, Türkiye, [2]Department of Medical Services and Techniques, Vocational Higher School of Healthcare Studies, Mardin Artuklu University, Mardin, Türkiye, [3]Department of Medical Biology, Faculty of Medicine, Dicle University, Diyarbakir 21280, Türkiye
[1]https://orcid.org/0000-0002-2317-0489, [2]https://orcid.org/0000-0003-3758-0654, [3]https://orcid.org/0000-0001-6160-5626
✉: ckeskinoo@gmail.com

ABSTRACT
The usage of metallic nanoparticles are very common. Environmentally friendly approaches in obtaining nanoparticles attract a lot of attention because of their advantages. In this study, an easy and economical biosynthesis of silver nanoparticles (AgNPs) was made with the extract of *Celtis tournefortii* LAM. leaf. For the characterization of synthesized nanoparticles, Spectrophotometer (UV-vis), Transmission Electron Microscope (TEM), Field Emission Scan Electron Microscopy (FE-SEM), Atomic Power Microscopy (AFM), Electron Disperse X-ray (EDX) Fourier Transformation Infrared Spectroscopy (FT-IR), X-ray Diffraction (XRD), Thermogravimetric and Differential Thermal Analysis (TGA-DTA), Zeta Sizer and Zeta Potential Analysis data were used. As a result of the data analysis, it was determined that the AgNPs had a spherical appearance, an average size distribution of 4.8 nm, had a maximum absorbance at a wavelength of 482.13 nm, a crystal nanosize of 10.95 nm, and a surface charge of -21.6 mV. Inhibition activities of AgNPs on the growth of pathogenic strains were determined by the microdilution method. The results showed that the nanoparticles were effective even at low concentrations. The Minimum Inhibitory Concentration (MIC) value of the tested materials on the growth of the strains was found between 0.03-1.00 µg mL^{-1}. Anticancer activity of AgNPs was investigated on CaCo-2, U118, Skov3 cancer cell lines and healthy cell line HDF by the MTT method.

Biology

Research Article

Article History
Received : 14.12.2021
Accepted : 18.02.2022

Keywords
AgNPs
Antimicrobial
Anticancer
Nanomedicine
FE-SEM

Celtis tournefortii LAM. Yaprak Özütüyle Gümüş Nanopartiküllerin Hızlı Biyosentezi; Antimikrobiyal ve Antikanser Aktivitelerinin İncelenmesi

ÖZET
Metalik nanopartiküllerin kullanım alanları çok yaygındır. Nanopartiküllerin elde edilmesinde çevre dostu yaklaşımlar getirdiği avantajlar ile oldukça fazla ilgi görmektedir. Bu çalışmada, Celtis tournefortii LAM yaprağı özütü ile gümüş nanopartiküllerin (AgNP'ler) kolay ve ekonomik bir biyosentezi yapıldı. Sentez ile elde edilen nanopartiküllerin karakterizasyonu için Spektrofotometre (UV-vis), Geçirmeli Elektron Mikroskopu (TEM), Alan Emisyon Taramalı Elektron Mikroskobu (FE-SEM), Atomik Güç Mikroskopisi (AFM), Enerji Dağılımlı X-Ray Floresans Spektrometre Cihazı (EDX), Fourier dönüşüm kızılötesi spektroskopisi (FT-IR), X-ışını difraksiyon (XRD), termogravimetrik ve diferansiyel termal analizi (TGA-DTA), Zetasizer ve zeta potansiyeli analiz verileri kullanıldı. Analiz verileri sonucunda AgNP'lerin küresel bir görünüme sahip olduğu, ortalama boyut dağılımının 4.8 nm olduğu, 482.13 nm dalga boyunda maksimum absorbansa, 10.95 nm kristal nano boyutuna ve -21.6 mV yüzey yüküne sahip olduğu belirlendi. AgNP'lerin patojen suşların üremesi üzerindeki inhibisyon aktiviteleri mikrodilusyon yöntemi ile belirlendi. Elde edilen sonuçlar nanopartiküllerin düşük konsantrasyonlarda bile etkili olduklarını gösterdi. Test edilen

Biyoloji

Araştırma Makalesi

Makale Tarihçesi
Geliş Tarihi : 14.12.2021
Kabul Tarihi : 18.02.2022

Anahtar Kelimeler
AgNP'ler
Antimikrobiyal
Antikanser
Nanotıp
FE-SEM

materyallerin suşların büyümesi üzerindeki Minimum İnhibitör Konsantrasyon (MIC) değeri 0.03-1.00 µg mL^{-1} arasında bulundu. AgNP'lerin antikanser aktivitesi, MTT yöntemi ile CaCo2, U118, Skov3 kanser hücre hatları ve sağlıklı hücre hattı HDF üzerinde araştırıldı.

Atıf Şekli: Baran A, Keskin C, Kandemir SI 2022. *Celtis tournefortii* LAM. Yaprak Özütüyle Gümüş Nanopartiküllerin Hızlı Biyosentezi; Antimikrobiyal ve Antikanser Aktivitelerinin İncelenmesi. KSÜ Tarım ve Doğa Derg 25 (4): 72-84. https://doi.org/10.18016/ksutarimdoga.vi. 1036488

To Cite : Baran A, Keskin C, Kandemir SI 2022. Rapid Biosynthesis of Silver Nanoparticles by *Celtis tournefortii* LAM. Leaf Extract; Investigation of Antimicrobial and Anticancer Activities. Manuscript Title. KSU J. Agric Nat 25 (4): 72-84. https://doi.org/10.18016/ksutarimdoga.vi.1036488

INTRODUCTION

Particles between 1-100 nm are known as nanoparticles (NPs) (Kumar et al., 2017). These particles have a large surface area, superior physical and chemical properties. Among the metallic nanoparticles, Silver (Ag) (Baran 2019a), Gold (Au) (Baran 2020 et al., ; Keskin et al., 2021), Zinc (Zn) (Doğaroğlu et al., 2019), Titanium (Ti) (Baran et al., 2019b) are the commonly used ones. Among these metallic nanoparticles, AgNPs are used in many nanomedical applications, such as anticancer (Abu-Dief et al., 2020), anti-inflammatory (Kumar et al., 2019), antimicrobial (Mohammadi et al., 2019), antioxidant agent (Khalil et al., 2019). In addition, AgNPs can be used in bioremediation applications (Francis et al., 2017), in catalysis studies (Thomas et al., 2018), in cosmetics (Arroyo et al., 2020), and in many different areas including the food industry (Velmurugan et al., 2014). The AgNPs can be obtained by various methods. Among these methods physical, chemical and environmentally friendly biological methods are most used. Biological methods offer several advantages over physical and chemical methods, such as being environmentally friendly, low in cost, and not using toxic chemicals in the synthesis stages (Patil et al., 2018; Rolim et al., 2019). Synthesis studies made by plant sources among biological methods, besides the ease of processing and do not require special conditions stand out with synthesizing more products. (Al-ogaidi et al., 2017).

Antibiotic resistance is an important problem and numberless used antibiotics for treatment are unfortunately ineffective on microorganisms. The development resistance of microorganisms to antibiotics also increases the needing for new effective antimicrobial agents. The antimicrobial effects of AgNPs obtained by environmentally friendly synthesis methods have been demonstrated in many studies (Singh et al., 2018; Baran, 2018; Oliveira et al., 2019; Baran 2019a; Mohammadi et al., 2019; Aktepe et al., 2021a).

Cancer is one of the common diseases of the age and the treatment process is very troublesome. New treatment methods and the discovery of new anticancer agents for this disease are continued. There are some studies on the usability of AgNPs as anticancer agents. (Remya et al., 2015; Sarkar et al., 2018; Satpathy et al., 2018; Pandiyan et al., 2019; Baran et al., 2021; Gomes et al., 2021).

Celtis tournefortii, known as "Eastern fenugreek, Dardağan, Dıgdıge, Taok, Ingires or Dağdağan", is a deciduous tree species that grows in high temperate, tropical regions, and grows in high temperate, tropical regions. It grows in countries such as Turkey, Greece, Croatia, Iran, Ukraine, Iraq, and Azerbaijan. The edible fruits of the tree are often consumed in these countries. *Celtis tournefortii* fruit is used in traditional folk medicine for shortness of breath, chest pain, strengthening and polishing tooth, and healing wound (Ural, 2001; Keser et al., 2017; Kawarty et al., 2020). Studies on the *Celtis* genus reported that have many phytochemicals such as coumarins, tannins, flavonoids, terpenoids, alkaloids, coumaroyl tyramines, steroids, and phenolics are included in their chemical profile (Keser et al., 2017; Yıldırım et al., 2017; Gecibesler 2019). Phenolic compounds show antioxidant activity through the OH groups in their structures. In addition to their antioxidant properties; they have antiallergenic, antimutagenic, anticarcinogenic, antimicrobial, anti-inflammatory and antithrombotic effects. In addition, it is stated that regular nutrition with foods containing high levels of flavonoids reduces the incidence of diseases such as prostate and breast cancer in the society (Demir and Akpınar, 2020).

This study was aimed to synthesize and characterization of the AgNPs with the extract of *Celtis tournefortii* leaves and to determine their antimicrobial and anticancer effects.

MATERIAL and METHOD

Preparation of Plant Extract and Silver Nitrate Solution

Plant leaves (Figure 1B) were collected from Mardin Kızıltepe Region (37°17' 07.3" N and 40° 29' 03.0" E) (Figure 1A) at the end of the summer period (end of August). Plant samples were identified by Dr Cumali KESKİN. Plant samples were washed several times using tap water and then distilled water and it was dried in room condition. 100 grams of dried plant

samples were placed in a flask containing 500 ml of distilled water and allowed to boil. The obtained extract was cooled at room conditions and filtered for the using synthesis of nanoparticles.

Biosynthesis of AgNPs

A solution with a concentration of five millimolar (mM) was prepared from silver nitrate ($AgNO_3$; Sigma Aldrich) salt for the biosynthesis of AgNPs.

100 ml plant extract and 100 ml AgNO3 solution were mixed in a flask. The time depending colour changes were observed at the synthesizing period. To evaluate the formation and presence of AgNPs depending on the color change, samples were taken and wavelength scans were performed to determine the maximum absorbances with the UV-vis spectrophotometer.

Characterization of AgNPs

To detect the formation and presence of AgNPs, samples were taken with the color change due to the reaction, and the maximum absorbance values were examined by scanning in the wavelength range of 200-800 nm using the UV-vis Spectrophotometer (Perkin Elmer One). With FT-IR (Perkin Elmer One) spectroscopy, the spectrum changes of the frequencies of the extract and the reaction liquid obtained after the synthesis in the range of 4000-400 cm-1 were evaluated to determine the functional groups responsible for biosynthesis. The XRD (Rigaku Miniflex 600) device was used to determine the crystal patterns and sizes of synthesized AgNPs at 2θ in the range of 20-80. The below Debye-Scherrer equation was used to compute the crystal sizes (Baran 2018; Baran et al., 2020).

$$D = K\lambda / (\beta \cos\theta) \quad \text{(Eq. 1)}$$

(D = particle size, K = constant value, λ = X-ray wavelength value, β = half of the FWHM value of the maximum peak, θ = Bragg angle of the high peak).

SEM (EVO 40 LEQ), FE-SEM, TEM (Jeol Jem 1010) microscopes were used to determine the morphological appearance of AgNPs as a result of biosynthesis. In addition, the shape and topographic distributions of AgNPs were also shown with micrographs acquired by the AFM (Park System XE-100) device. Elemental compositions of the synthesized particles were evaluated using EDX (RadB-DMAX II computer-controlled) device data. The resistance of AgNPs to heat treatment was determined by thermogravimetric and differential thermal analysis (TG-DTA) are performed on DTG-60H Simultaneous DTA-TG Apparatus Shimadzu. The samples were heated to 25-900 °C at the rate of 10 °C min-1, individually in the atmosphere of dry air and N_2(g) flow rate of 20 cm^3/min. Zeta potential and zeta sizer analysis (Malvern, UK) data were also used to determine the surface charges and size distributions of AgNPs.

Antimicrobial Activities of AgNPs

The antimicrobial activities of synthesized AgNPs were determined against the growth of the pathogenic strains by the microdilution method. Gram positive bacteria *Bacillus subtilis* ATCC 11774 (*B. subtilis*) and *Staphylococcus aureus* ATCC 29213 (*S. aureus*), gram negative bacteria *Pseudomonas aeruginosa* ATCC27833 (*P. aeruginosa*) and *Escherichia coli* (*E. coli*) ATCC25922 were used for MIC assay. In addition, the antifungal effect of AgNPs was determined on *Candida albicans* (*C. albicans*) yeast with the same method. The *C. albicans*, *S. aureus*, and *E. coli* microorganisms were procured from İnönü University Medical Faculty Hospital Microbiology Laboratory (in Malatya, Turkey), and B. subtilis and P. aeruginosa microorganisms were procured from Mardin Artuklu University Microbiology Research Laboratory (Mardin, Turkey).

Gram-positive and gram-negative bacteria (Nutrient agar) and yeast (Sabora dextrose agar) were incubated in the growing medium at 37 °C overnight. McFarland solution was prepared with a turbidity value of 0.5 by using bacteria and yeast strains grown on the medium plates (Emmanuel et al., 2015). Then, Mueller-Hinton Broth (bacteria) and Roswell Park Memorial Institute 1640 broth (yeast) medium were transferred to 96 well microplates in appropriate amounts for microorganisms. Some wells were designated for sterilization and control steps. Solutions containing AgNPs at different concentrations were prepared and transferred into microplates. Afterwards, a series of micro dilutions were applied to the wells to ensure the distribution of AgNPs in the medium. After this process, microorganism solutions prepared according to McFarland 0.5 were added into the microplate wells. At the end of the administration, the prepared microplates were kept in incubation at 37 °C for one night. After the incubation period, the microplates were examined for the growth of microorganisms. The concentration of the well where growth occurred was determined as the MIC value.

Anticancer Effects of AgNPs

Anticancer effects of AgNPs obtained by biosynthesis were carried out in Dicle University Scientific Research Center, Cell Culture Laboratory (Diyarbakir, Turkey), using the MTT method. Cell lines used in the experimental application were obtained from the American Type Culture Collection (ATCC). The cytotoxic effects on Glioblastoma (U118), Human Colorectal Adenocarcinoma (Caco-2), Human Ovarian sarcoma (Skov-3) cancer cell lines used in the application, as well as on healthy cell line Human Dermal Fibroblast (HDF) cell lines were investigated.

CaCo2, U118, and HDF cell lines were grown in 75 t-flasks in Dulbecco's Modified Eagle (DMEM) medium containing 2 mM L-Glutamine, 10% FBS, 100 U/ml Penstrep. The Skov-3 cell line was also grown in RPMI media with 10% FBS, 100 U/ml Penstrep in 75 t-flasks. The flasks of the cultured cell lines were kept in an oven at 37 °C with 5% CO_2, 95% air, and humidity conditions for cell growth. Then, it was examined whether the cell lines were at 80% confluence with a hemocytometer and resuspended at different concentrations. Suspended cell lines were transferred to 96-well microplates and incubated overnight. At the end of the period, AgNPs with concentrations ranging from 25 µg ml^{-1} to 200 µg ml^{-1} were added to the wells cultured with cell lines and allowed to interact for 48 hours. After the interaction period, MTT solution was added to the microplate wells and waited for 3 hours. Then DMSO (Dimethyl sulfoxide) was added and waited for 15 minutes. After these procedures, the absorbance data of the cells were evaluated at a wavelength of 540 nm by the MultiScan Go, Thermo device. The Absorbance values of the cell lines and the concentrations of AgNPs that suppressed the % viability on the cell lines were calculated using Equation 2 given below (Remya et al., 2015)

$$\%viability = U/C*100 \quad (2)$$

In the equation, U; The absorbance values of the cells after interaction with AgNPs, C; represents the absorbance values of control cells.

RESULT and DISCUSSION

UV-vis spectrophotometric data

A rapid color changes off yellow to brown were observed after the 5 minutes from mixing solution. This color change and the 482.13 nm maximum absorbance bands (Figure 1) that show surface plasma resonance vibrations (SPR) due to the formation of AgNPs are characteristic data of AgNPs (Luna et al., 2015; Eren and Baran 2019).

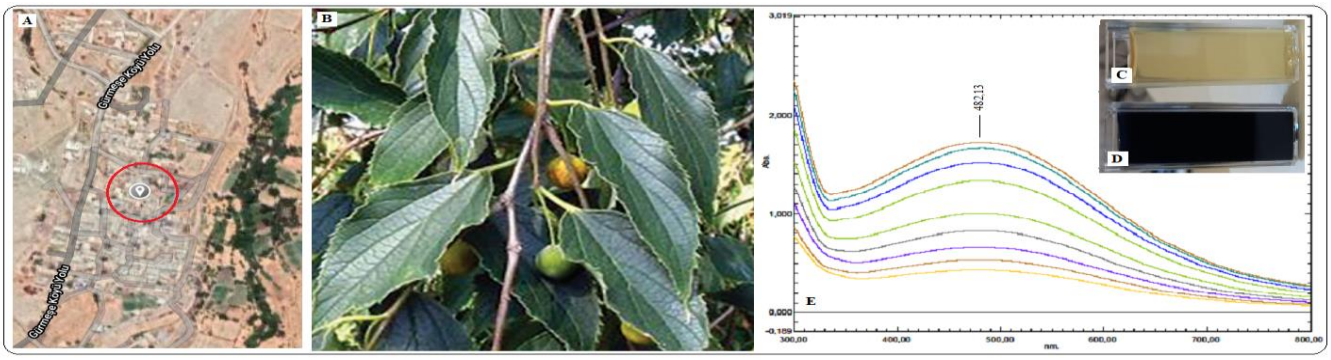

Figure 1. A. *C. tournefortii* geographical location of the growing area, **B**. leaves of the plant, **C.** plant extract image, **D**. color change as a result of the synthesis of AgNPs, and **E**. UV-vis Spectrophotometric data showing the presence of AgNPs

Şekil 1. **A**. *C. tournefortii*'nin yetiştiği alana ait coğrafi konum, **B**. bitkinin yaprakları, **C.** bitki özütü görüntüsü, **D**. AgNP'lerin sentezi sonucunda meydana gelen renk değişimi ve **E.** AgNP'lerin varlığını gösteren UV-vis spektrofotometrik verileri

XRD analysis

XRD analysis data performed to evaluate the crystal pattern and dimensions of AgNPs, the spectra were taken at 111°, 200°, 220°, and 311° at 2θ. The values of these spectra determined as 38.06, 44.35, 64.35, and 77.26 respectively (Figure 2). XRD data show that the crystal pattern of AgNPs are cubic and they have 10.95 nm crystal size. (Krishnaraj et al., 2010; Patra et al., 2016; Rani et al., 2020).

FTIR analysis

FTIR spectra of the plant extract and the reaction liquid after synthesis were used in the evaluation of the functional groups of phytochemicals that may be responsible for the reduction of the Ag^+ form to the Ag^o form. Frequency shift was detected at three points (Figure 3). The shifts in the FTIR spectrum at 3337. 81-3330. 20 cm^{-1}, 2122. 95-2122. 80 cm^{-1}, and 1635. 48-1635. 33 cm^{-1} are due to the bioreduction of hydroxyl groups (O-H stretch), aromatic groups (C=C stretch), flavonoid and phenolic groups (C=O stretching) has shown to be effective (Kumar et al., 2015; Khan et al., 2018; Hemmati et al., 2019; Jebril et al., 2020). In addition, the frequency shift occurring at 163548 cm^{-1} showed the effectiveness of proteins as a capping agent in AgNPs in ensuring the stability of AgNPs in synthesis (Hemmati et al., 2019).

FESEM and TEM micrographs of AgNPs

The images of the morphological appearances of AgNPs in FE-SEM and TEM micrographs were determined. As seen in Figure 4, TEM and FESEM micrographs showed that AgNPs exhibited a spherical appearance (Kumar et al., 2016, Othman et al., 2017, Thomas et al., 2018, Wongpreecha et al., 2018). AgNPs were evaluated to have an average size

of 5.28-10.80 nm in TEM micrographs (Gopinath et al., 2016; Atalar et al., 2021).

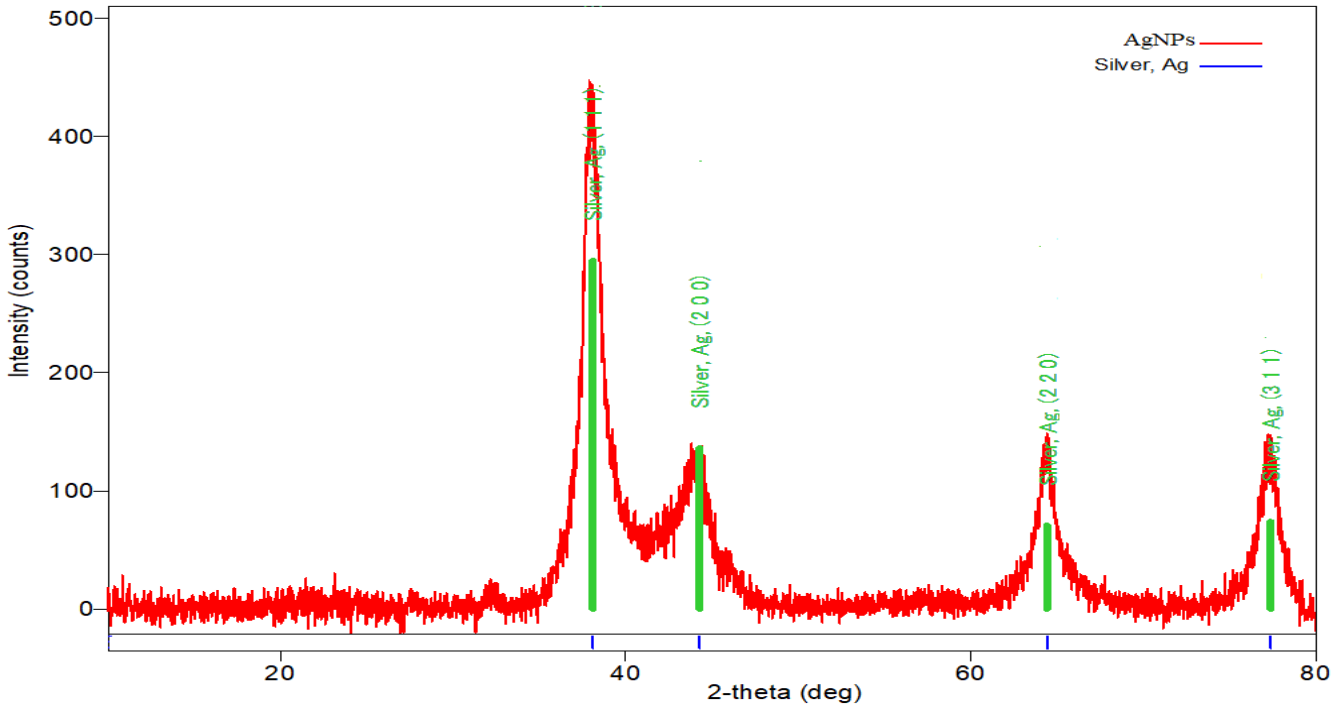

Figure 2. X-ray diffraction of the crystal patterns of biosynthesized AgNPs
Şekil 2. *Biyosentezi yapılan AgNPlerin kristal desenlerine ait X-ray diffractionu*

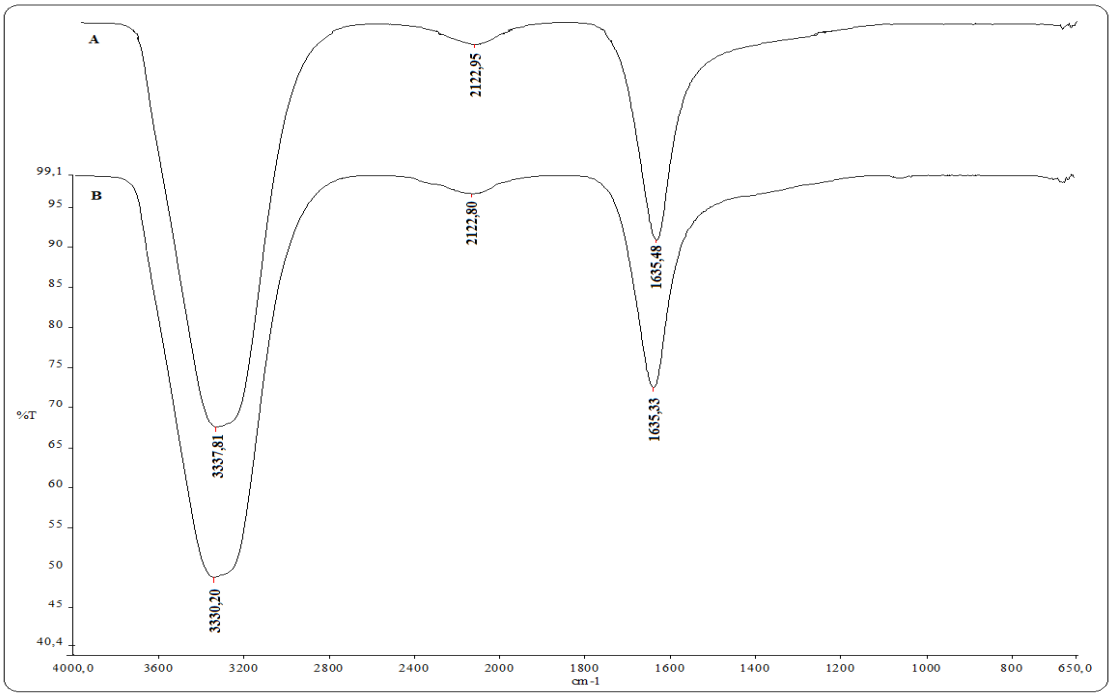

Figure 3. FTIR spectra of *C. tournefortii* plant extract **(A)** and reaction liquid obtained as a result of Synthesis **(B)**
Şekil 3. *FTIR spektrumları; **A.** C. tournefortii bitki özütü ve **B.** Sentez sonucunda elde edilen reaksiyon sıvılarının ait*

EDX analysis

EDX data was used for the evaluation of the elemental compositions of nanoparticles synthesized with *C. tournefortii* leaf extract. It was determined that almost all of the particles were formed by AgNPs with the presence of strong peaks belonging to the silver field (Pallela et al., 2018). The low peaks of elements such as carbon and oxygen are due to the phytochemicals in the plant extract, which act as a capping agent that provides stability on the surface of AgNPs (Vastrad 2016; Kumar et al., 2019; Das et al., 2021). The frequency shifts in the FTIR spectra in Figure 3 also supports this situation.

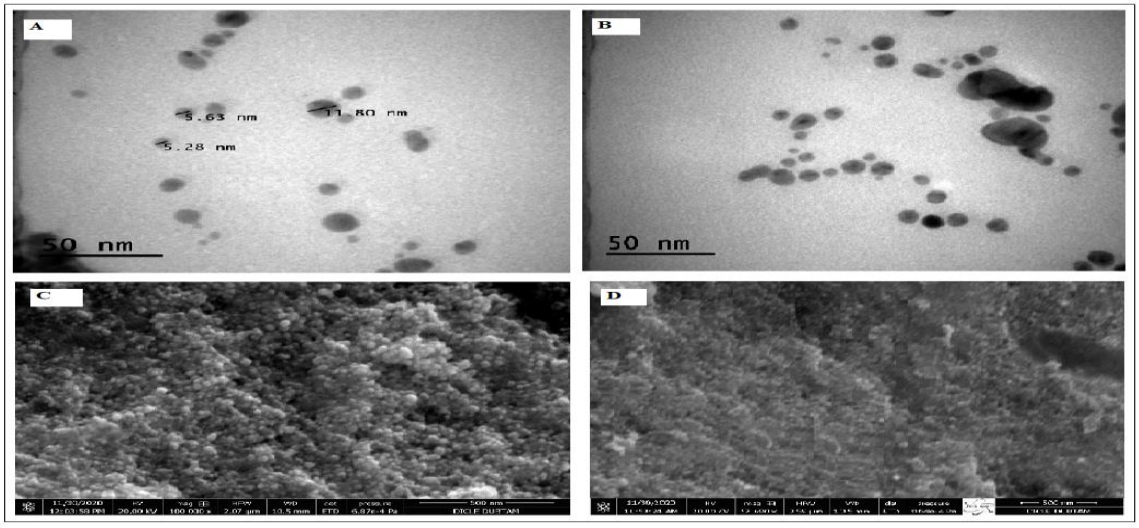

Figure 4. Morphological appearances of AgNPs after biosynthesis with *C. tournefortii* leaf extract; **A** and **B** TEM, **C** and **D** FESEM micrographs

Şekil 4. *C. tournefortii yaprak özütü ile biyosentez sonrası AgNP'lerin morfolojik görünümleri; **A** ve **B** TEM, **C** ve **D** FESEM mikrografları*

TGA-DTA analysis

TGA-DTA data obtained at 25-1000 °C was used to determine the resistance of AgNPs to temperature changes. In the graphics, it was seen that 2.47%, 9.38% and 6.38% mass losses occurred at 18.4 °C, 423.72 °C and 878.41 °C, respectively (Figure 5). The first mass loss is due to the loss of water adsorbed at 18.4 °C. The second mass loss at 423.72 °C and the third at 878.41 °C is due to the phytochemicals found on the surface of AgNPs (Baran 2019c; Rolim et al., 2019; Keskin et al., 2021). The weak C and O peaks in the EDX profile in Figure 6 also confirm this situation.

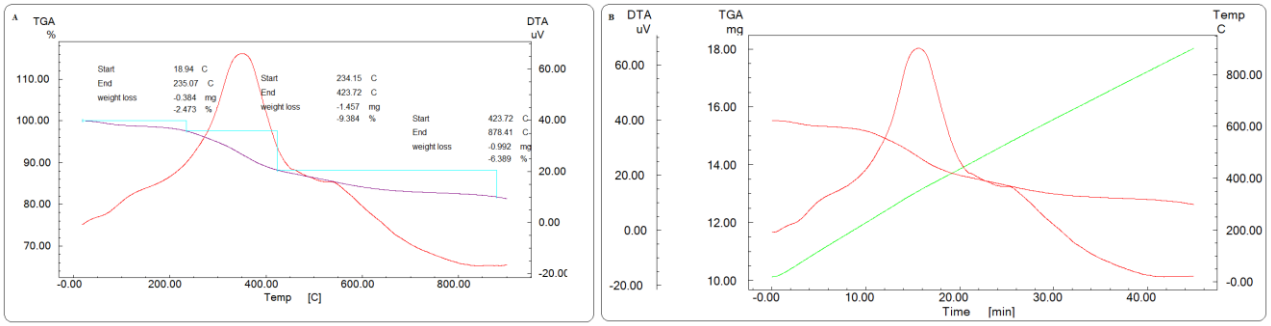

Figure 5. AgNPs Thermal resistance temperature points with **A** and **B** TGA-DTA data of AgNPs after biosynthesis

Şekil 5. *Biyosentez sonrası AgNP'lerin **A** ve **B** TGA-DTA datalarıyla termal direnç sıcaklık noktaları*

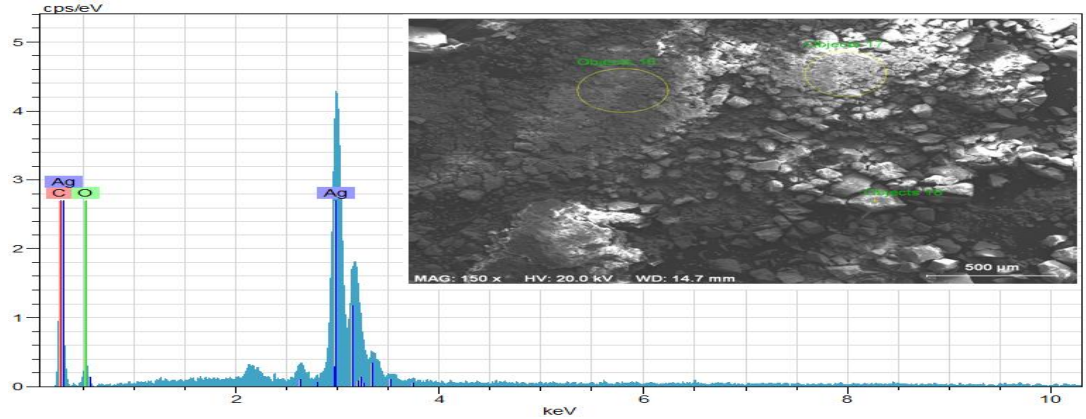

Figure 6. EDX profile of elemental compositions of post-biosynthesis particles with *C. tournefortii* plant extract

Şekil 6. *C. tournefortii* bitki özütü ile biyosentez sonrası partiküllerin element kompozisyonlarının EDX profili

Zeta size and zeta potential distributions of AgNPs

The zeta size and zeta potential analyses were performed to determine the surface charges and size distributions of the biosynthesized AgNPs, it was determined that AgNPs has an average size distribution of 4.8 nm and a surface charge of -21.6 mV. (Figures 7A and 7B). There is no standard size in nanoparticle synthesis, different sizes of nanoparticles can be synthesized. Remya et al., 2015, Alkhulaifi et al., 2020, and Singh et al., 2018 reported the average nanoparticle sizes as 27-32 nm, 59.74 nm and 5-10 nm, respectively. On the other hand, synthesized AgNPs exhibit only negative charge distribution is important data showing that AgNPs are stable. Green way synthesized AgNPs show better negative charge distribution compared to conventional (Chemical and physical way) synthesis studies. In this polymer matrix, the presence of oxidized hydroxyl groups of free electrons is the factor that makes the system more stable in colloidal form. The negative charge distribution is due to the phytochemicals present on the surface of AgNPs (Pugazhendhi et al., 2018; Oliveira et al., 2019; Jebril et al., 2020). The results of FTIR spectra, EDX profile, and TGA-DTA graphs given in Figure 3, Figure 5, Figure 6, support this data. The different surface charges of AgNPs cause problems such as fluctuation and aggregation due to electrostatic attraction between nanoparticles (Al-ogaidi et al., 2017; Satpathy et al., 2018) and this situation negatively affects their stable structure (Al-ogaidi et al., 2017; Satpathy et al., 2018; Patil et al., 2018). AgNPs obtained by biosynthesis exhibited a stable structure with the surface charge distribution of -21.6 mV. In other studies reported that the obtained AgNPs show -19 mV (Al-ogaidi et al., 2017; Oliveira et al., 2019) and −22 ± 5 mV (Ferreyra Maillard et al., 2018) zeta potential distribution.

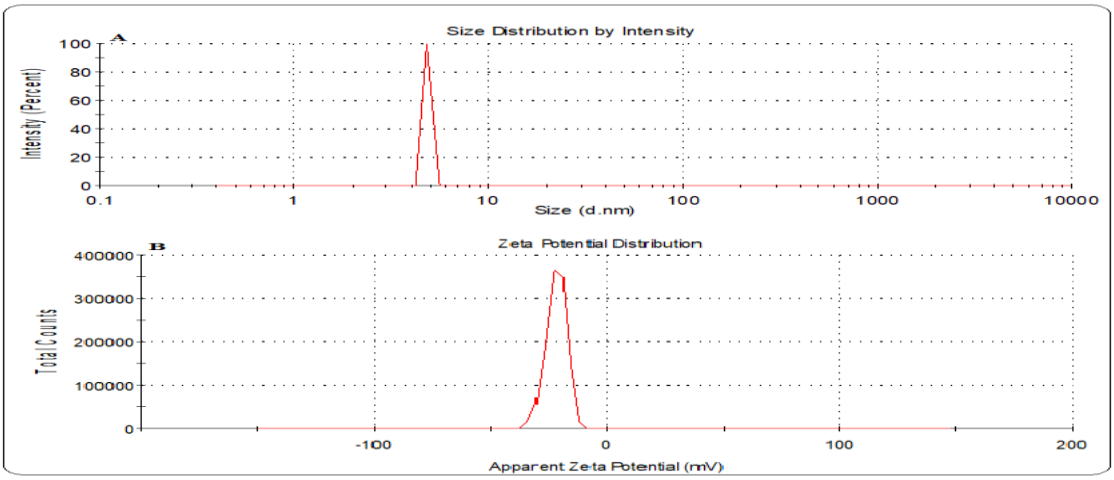

Figure 7. AgNPs after biosynthesis; A. Density-dependent size distribution, B. Zeta potential charge distribution graphs

Şekil 7. *Biyosentez sonrası AgNPlerin; A. Yoğunluğa bağlı boyut dağılımı, B. Zeta potansiyeli yük dağılımı grafikleri*

AFM micrographs of AgNPs

Topographic distributions and structures of the biosynthesized AgNPs were evaluated by AFM. As seen in Figure 8, it was seen that AgNPs were spherical, showed monodisperse properties and had dimensions below 15 nm (Swamy et al., 2015; Kumar et al., 2017; Rauf et al., 2021).

Antimicrobial effects of AgNPs

The effects of AgNPs synthesized with *C. tournefortii* leaf extract on pathogen strains were determined by defining MIC by the microdilution method. To compare this effect, the same application steps were performed in standard antibiotics and $AgNO_3$ solution. The data show that concentrations of 0.03-1.00 µg mL-1 have a suppressive effect on the growth of microorganisms (Table 1 and Figure 9). 0.06-0.13 µg mL^{-1} and 0.50-1.00 µg mL^{-1} AgNPs concentrations showed effective suppressor activity on gram-positive *B. subtilis*, *S. aureus* and gram-negative bacteria *P. aeruginosa*, *E. coli* respectively. AgNPs showed effectiveness on *C. albicans* growth with 0.03 µg mL^{-1} at a much lower concentration than antibiotics and silver nitrate solution. AgNPs are ionized in a liquid medium and tend to show high reactivity. After being ionized in the aqueous environment, they interact with the microorganisms in the same environment depending on the electrostatic attraction force (Narayan and Dipak 2015; Ahmed et al., 2016; Aina et al., 2018). After the interaction, they cause an increase in reactive oxygen species (ROS) within the microorganisms. Biomolecules with a high affinity for ROS (such as cell membrane, DNA, RNA, some enzymes) are adversely affected by this situation. The functions and structure of adversely affected

biomolecules are impaired. Due to these reasons, the death of the microorganism occurs (Emmanuel et al., 2015; Shao et al., 2018). In Table 2, some biosynthesis studies using the green synthesis method are given.

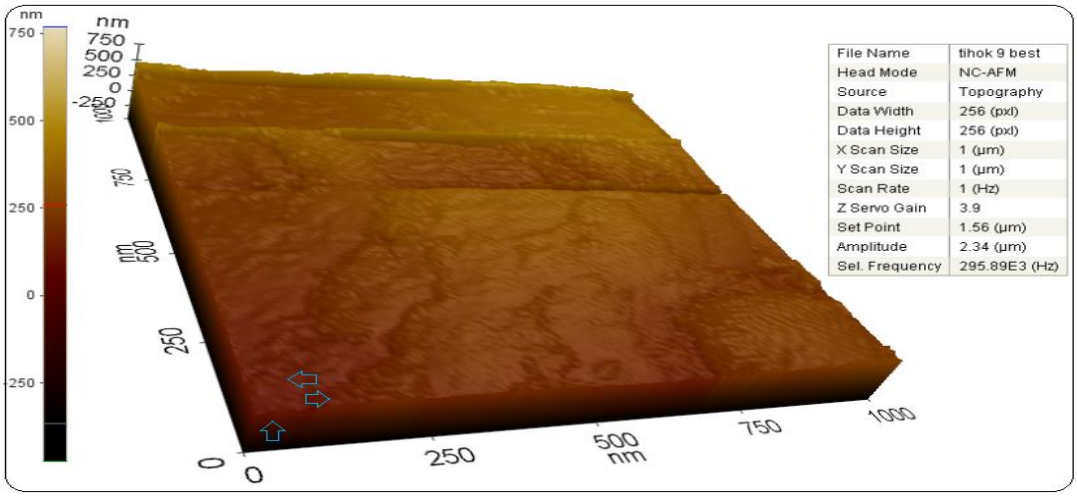

Figure 8. AFM micrograph of topographic structures and shapes of AgNPs
Şekil 8. AgNP'lerin topografik yapı ve şekilerinin AFM mikrografisi

Table 1. Antimicrobial effect concentrations of AgNPs, antibiotics and silver nitrate solution on the growth of microorganisms
Tablo 1. *AgNP'lerin, antibiyotiklerin ve gümüş nitrat çözeltisinin mikroorganizmaların üremeleri üzerinde antimikrobiyal etki gösterdikleri konsantrasyonları*

TESTED ORGANISM	AgNPs µg mL^{-1}	Silver Nitrate µg mL^{-1}	Antibiotic µg mL^{-1}
S. aureus	0.13	2.00	2.00
B. subtilis	0.06	1.00	0.50
E. coli	1.00	4.00	4.00
P. aeruginosa	0.50	2.00	4.00
C. albicans	0.03	0.50	1.00

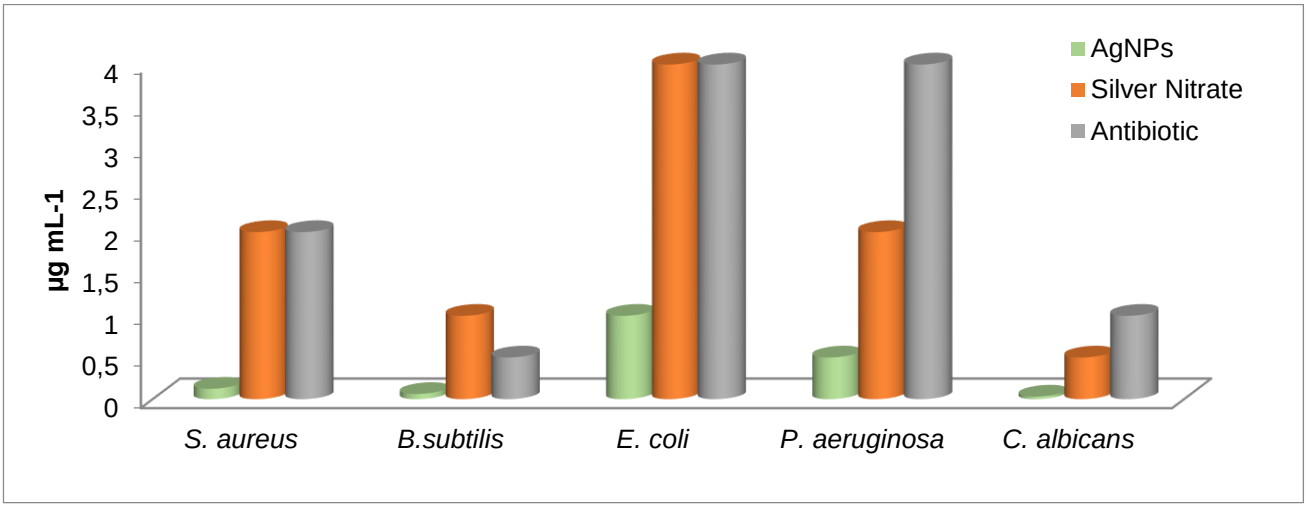

Figure 9. Comparison of Antimicrobial Effects of AgNPs with $AgNO_3$ and antibiotics
Şekil 9. AgNP'lerin Antimikrobiyal etiklerinin $AgNO_3$ ve antibiyotiklerle karşılaştırılması

Anticancer Effects of AgNPs

The most important advantage of plant-based synthesis is that there is no need to use chemicals. Phytochemicals (phenols, amines, flavonoids, terpenes), especially phenolic compounds, in their structure facilitate the synthesis. In addition, these phytochemicals can be shown as the source of many other biological activities of nanoparticles. The functional groups of these phytochemicals surrounding nanoparticles are preferred in anticancer studies due to their bonding properties (Demir at al., 2020; Aktepe et al., 2021b). The viability-suppressing

effects of biosynthesized AgNPs were investigated using the MTT (3-(4,5-Dimethylthiazol-2-yl)-2,5-Diphenyl tetrazolium Bromide) method on U118, CaCo-2, and Skov-3 cancer cell lines and healthy cell line HDF. As seen in Table 3 and Figure 10, AgNPs have a very low toxic effect on healthy cell line HDF at a concentration of 25 µg mL^{-1} with a viability rate of 79.45%. In cancer cell lines, it was observed that it was most effective on the CaCo-2 cell line with an inhibition rate of 58.99%. On the U118, Skov-3 cell lines, it was determined that the viability rate of 24.83% and 30.86%, respectively, was suppressed at 200 µg mL^{-1} concentration.

Table 2. Antimicrobial effects of AgNPs obtained by biosynthesis in green synthesis studies
Tablo 2. *Green sentez çalışmalarında elde edilen AgNP'lerin antimikrobiyal etkileri*

Biological Source	Average Size (nm)	Gram-Negative µg mL^{-1}	Gram-Positive µg mL^{-1}	References
Camellia sinensis	23	7-30	30-250	(Rolim et al., 2019)
Chitosan	>20	39.1	312.5	(Wongpreecha et al., 2018)
Fritillaria	10	2-8	1-4	(Hemmati et al., 2019)
Citrullus lanatus	21.27	0.13-0.25	0.50-1.00	(Aktepe and Baran, 2021a)
Acalypha indica	20-30	10	10	(Krishnaraj et al., 2010)
Hawthorn leaf	16.50	0.11	0.25	(Baran, 2019b)
Madhuca longifolia	30-50	80-90	40-60	(Patil et al., 2018)
Abelmoschus esculentus	19.05	0.12-0.50	0. 03-0.12	(Hatipoğlu, 2021)
Prunus amygdalus L. (almond)	14.67	1.00-2.00	0.13	(Aktepe and Baran 2021b)
Pistacia terebinthus	15	0.8	0.32	(Baran 2018)
C. tournefortii leaf extract	10	0.06-0.13	0.50-1.00	This study

Table 3. % viability rates as a result of interactions of AgNPs with cell lines
Tablo 3. *Hücre hatlarının AgNP'lerle etkileşimleri sonucunda % canlılık oranları*

Cell Line	25 µg mL-1	50 µg mL-1	100 µg mL-1	200 µg mL-1
HDF	79.45	67.55	67.55	41.00
U118	93.93	84.57	78.86	75.17
CaCo-2	41.01	34.22	32.42	26.69
Skov-3	100	95.76	90.88	69.14

The AgNPs have high oxidative effects and tend to settle on some biomolecules (such as cell membrane, nucleus). They are localized to these biomolecules and cause toxic effects by causing damage to biomolecules with the increase of ROS, and also by stimulating apoptosis and directing the cell to death (Gliga et al., 2014; Remya et al., 2015; Morais et al., 2020). As a result of these effects, the toxic effects of Ag^{+} ions released in living environments should be examined and evaluated (Wongpreecha et al., 2018). Some properties of nanomaterials play a decisive role in their toxic effect. These include properties such as concentration, shape, charge, exposure time, chemistry of the surface composition, degree of deposition, and size (Rolim et al., 2019).

In environmentally friendly synthesis studies, it has been stated that AgNPs have toxic effects on CaCo-2 from cancer cell lines at concentrations of 3.75 µg mL^{-1} (Mohmed et al., 2017) and 5 µg mL-1 (Zein et al., 2020) in suppressing viability. In studies with HDF and Skov-3 cells, it was stated that 25 µg mL-1 concentration suppressed the viability of the cells (Aktepe et al., 2021a; Baran et al., 2021). Various properties of nanoparticles such as interaction times, sizes, surface charges, concentrations, shapes, deposition degrees play a role in determining their toxic activities (Remya et al., 2015; Swamy et al., 2015).

CONCLUSION

This is the first study on biomedical applications of silver nanoparticles obtained using *Celtis tournefortii* leaf extract. The biosynthesis of AgNPs was carried out in an environmentally friendly, easy and cost-effective way. The characteristic properties of the synthesized AgNPs were determined by UV-vis, FT-IR, FE-SEM, TEM, AFM, EDX, XRD, TGA-DTA, Zeta sizer, and Zeta potential analysis data. It was determined that AgNPs had an average size of 10 nm, a spherical morphological appearance, a maximum absorbance of 483.13 nm, and a surface charge of -21.16 mV. The results of analyzing data such as TGA-DTA, EDX, AFM showed that these AgNPs have only a negative charge with -21.6 mV and that AgNPs

have a stable structure. The Microdilution method was determined that synthesized AgNPs showed the antimicrobial effect on pathogen strains even at very low concentrations. The MTT assay data demonstrated the suppressive effect of AgNPs (25 µg mL^{-1}), especially on the CaCo-2 cancer cell line, with a survival rate of 58.995%. In addition, in the examinations of AgNPs to evaluate their toxic effect on healthy cells lines (HDF), it was seen that it has a quality that can eliminate the toxic effect concerns with its 79.45% viability rate when used as an anticancer agent. It is thought that the application steps of biosynthesized AgNPs will contribute to the search for antimicrobial and anticancer agents, especially in biomedical applications.

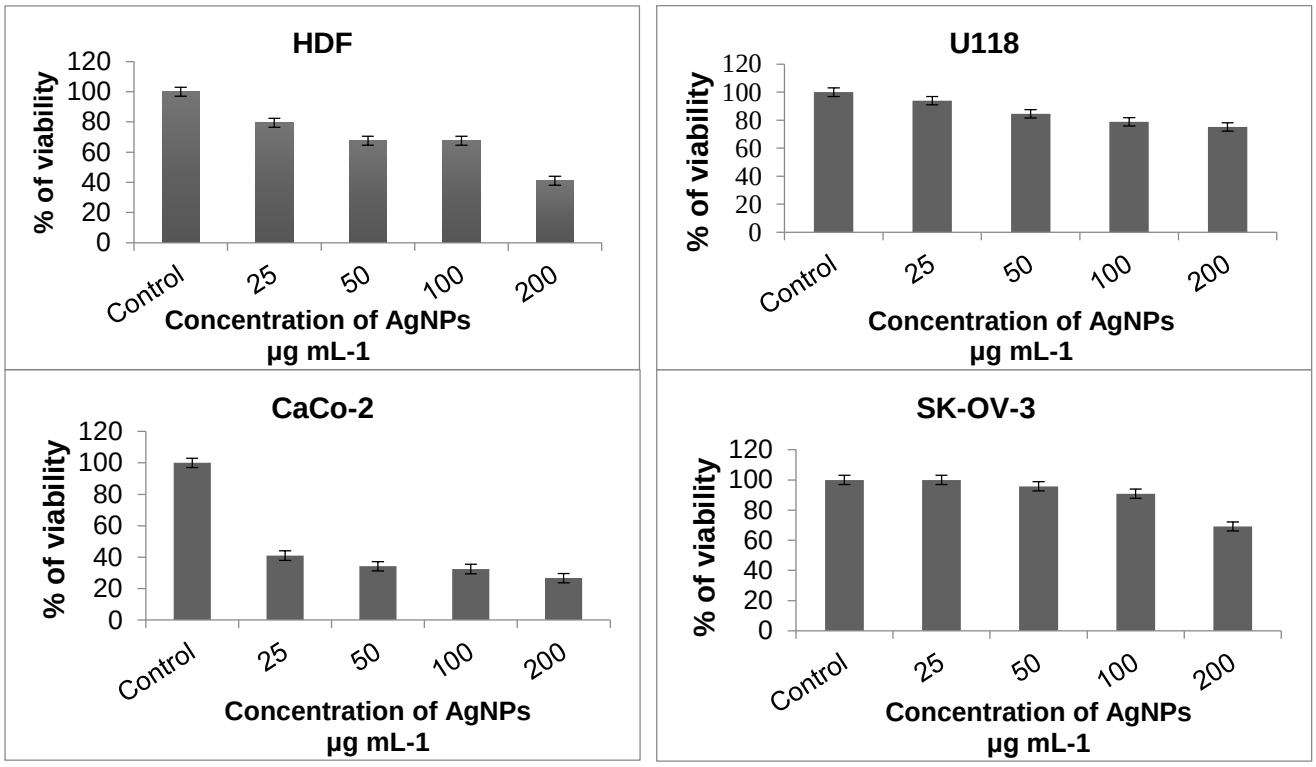

Figure 10. % viability rates resulting from the interaction of AgNPs on cell lines for 48 hours with the MTT method

Şekil 10. *AgNP'lerin MTT metoduyla hücre hatları üzerinde 48 saat etkileşimleri sonucu canlılık oranları*

ACKNOWLEDGEMENTS

This study was created by using some of the doctoral thesis data of Ayşe BARAN.

Statement of Conflict of Interest

The authors declare that there is no conflict of interest regarding the publication of this article.

Author's Contributions

The contribution of the authors is equal.

REFERENCES

Abu-Dief AM, Abdel-Rahman LH, Abd-El Sayed MA, Zikry MM, Nafady A 2020. Green Synthesis of AgNPs Utilizing Delonix Regia Extract as Anticancer and Antimicrobial Agents. ChemistrySelect 5(42): 13263–13268.

Ahmed KBA, Raman T, Veerappan A 2016. Future prospects of antibacterial metal nanoparticles as enzyme inhibitor. Mater. Sci. Eng. C 68: 939–947.

Aina AD, Owolo O, Adeoye-Isijola M, Aina FO, Favour O, Adewumi AG 2018. Almond leaves for the one-pot Biofabrication of silver nanoparticles: Characterization and larvicidal application. Int. J. Sci. Res. Publ. 8(11): 703–711.

Aktepe N, Baran A, Atalar MN, Baran MF, Keskin C., Düz MZ, Yavuz, Ö, İrtegün Kandemir S, Kavak DE 2021a. Biosynthesis of Black Mulberry Leaf Extract and Silver Nanoparticles (AgNPs): Characterization, Antimicrobial and Cytotoxic Activity Applications. MAS J. Appl. Sci. 8 (8): 685–700.

Aktepe N, Keskin C., Baran A, Atalar MN, Baran MF, Akmeşe Ş 2021b. Biochemical components, enzyme inhibitory, antioxidant and antimicrobial activities in endemic plant *Scilla mesopotamica speta*. J. Food Process. Preserv. 45 (11):e15980.

Aktepe N, Baran A 2021a. Biosynthesis of AgNPs by extract from waste leaves of *Citrullus lanatus* sp . (watermelon); characterization , antibacterial and antifungal effects. Prog. Nutr. 23 (3): e2021243.

Aktepe N, Baran A 2021b. Fast and Low-Cost Biosynthesis of AgNPs with Almond Leaves : Medical Applications with Biocompatible Structures. Prog. Nutr. 23 (9): e2021271.

Atalar MN, Baran A, Baran MF, Keskin C, Aktepe N, Yavuz Ö, İrtegun Kandemir S 2021. Economic fast synthesis of olive leaf extract and silver nanoparticles and biomedical applications. Part. Sci. Technol. 2021: 1–9.

Al-ogaidi I, Salman MI, Mohammad FI, Aguilar Z, Al-M, Hadi YA, Al-rhman RMA 2017. Antibacterial and Cytotoxicity of Silver Nanoparticles Synthesized in Green and Black Tea. World J. Exp. Biosci. 5(1): 39–45.

Alkhulaifi MM, Alshehri JH, Alwehaibi MA, Awad MA, Al-enazi NM, Aldosari NS, Hatamleh AA, Raouf NA 2020. Green synthesis of silver nanoparticles using *Citrus limon* peels and evaluation of their antibacterial and cytotoxic properties. Saudi J. Biol. Sci. 27(12): 3434–3441.

Arroyo G V., Madrid AT, Gavilanes AF, Naranjo B, Debut A, Arias MT, Angulo Y 2020. Green synthesis of silver nanoparticles for application in cosmetics. J. Environ. Sci. Heal. - Part A Toxic/Hazardous Subst. Environ. Eng. 55(11): 1304–1320.

Baran MF, Acay H, Keskin C, Aygün H, Yildirim A 2019b. Synthesis and Determination Of Antimicrobial Properties Of TiO_2NPs Using *Nigella sativa* L. Extract. EJONS Math. Eng. Nat. Med. Sci. 7: 69–75.

Baran MF 2018. Green Synthesis Of Silver Nanopartıcles (AgNPs) Usıng Pistacia terebinthus Leaf: Antimicrobial Effect And Characterization. EJONS Int. J. Math. Eng. Nat. Sci. 2 (2018): 67–75.

Baran MF. 2019a. Synthesis of silver nanoparticles (AgNP) with *Prunus avium* cherry leaf extract and investigation of its antimicrobial effect. Dicle Univ. J. Eng. 10(1): 221–227.

Baran MF 2019b Evaluation of Green Synthesis and Anti-Microbial Activities of AgNPs Using Leaf Extract of Hawthorn Plant. Res. Eval. Sci. Math. 3: 110–120.

Baran MF 2019c. Synthesıs , Characterization And Investigation of Antimicrobial Activity of Silver Nanoparticles From *Cydonia oblonga* Leaf. Applied Ecol. Env. Res. 17(2): 2583–2592.

Baran MF, Acay H, Keskin C. (2020). Determination of Antimicrobial and Toxic Metal Removal Activities of Plant-Based Synthesized (*Capsicum annuum* L. Leaves), Ecofriendly, Gold Nanomaterials. Glob Chall. 4(5), 1900104.

Baran A, Baran MF, Keskin C, Kandemir SI, Valiyeva M, Mehraliyeva S, Khalilov R, Eftekhari A 2021. Ecofriendly/Rapid Synthesis of Silver Nanoparticles Using Extract of Waste Parts of Artichoke (*Cynara scolymus* L.) and Evaluation of their Cytotoxic and Antibacterial Activities. J. Nanomater. 2021: 1–10

Das G, Shin H, Kumar A, Vishnuprasad CN 2021. Photo-mediated optimized synthesis of silver nanoparticles using the extracts of outer shell fibre of Cocos nucifera L . fruit and detection of its antioxidant , cytotoxicity and antibacterial potential. Saudi J. Biol. Sci. 28(1): 980–987.

Demir T, Akpınar Ö 2020. Biological Activities of Phytochemicals in Plants. Turkish JAF Sci.Tech. 8 (8): 1734-1746.

Demir T, Akpınar Ö, Kara H, Güngör H 2020. Cherry stem phenolic compounds: Optimization of extraction conditions and in vitro evaluations of antioxidant, antimicrobial, antidiabetic, anti-inflammatory, and cytotoxic activities. J Food Process Preserv. 44 (10):e14804.

Emmanuel R, Palanisamy S, Chen S, Chelladurai K, Padmavathy S, Saravanan M, Prakash P, Ali MA, Al-hemaid, Fahad MA 2015. Antimicrobial efficacy of green synthesized drug blended silver nanoparticles against dental caries and periodontal disease causing microorganisms. Mater. Sci. Eng. C 56: 374–379.

Doğaroğlu ZG, Eren A, and Baran MF. 2019. Effects of ZnO Nanoparticles and Ethylenediamine- N,N′ - Disuccinic Acid on Seed Germination of Four Different Plants. Glob. challanges 1800111: 1–5.

Eren A, Baran MF 2019. Green Synthesis , Characterızatıon And Antimicrobial Activity Of Silver Nanoparticles (AgNPs) From Maize (*Zea mays* L .). Applied Ecol. Env. Res. 17(2): 4097–4105.

Ferreyra Maillard APV, Dalmasso PR, López de Mishima BA, Hollmann A 2018. Interaction of green silver nanoparticles with model membranes: possible role in the antibacterial activity. Colloids Surfaces B Biointerfaces 171: 320–326.

Francis S, Joseph S, Koshy EP, Mathew B 2017. Green synthesis and characterization of gold and silver nanoparticles using *Mussaenda glabrata* leaf extract and their environmental applications to dye degradation. Environ. Sci. Pollut. Res. 24: 17347–17357.

Gecibesler IH 2019. Antioxidant Activity and Phenolic Profile of Turkish *Celtis tournefortii*. Chem. Nat. Compd. 55(4): 738–742.

Gliga AR, Skoglund S, Wallinder IO, Fadeel B, Karlsson HL 2014. Size-dependent cytotoxicity of silver nanoparticles in human lung cells: the role of cellular uptake, agglomeration and Ag release. Part. Fibre Toxicol. 11(1): 1–17.

Gomes, H. I. O., Martins, C. S. M., Prior, J. A. V. (2021). Silver Nanoparticles as Carriers of Anticancer Drugs for Efficient Target Treatment of Cancer Cells. Nanomater. 11(4), 964.

Gopinath K, Kumaraguru S, Bhakyaraj K, Mohan S, Venkatesh KS, Esakkirajan M, Kaleeswarran P,

Alharbi NS, Kadaikunnan S, Govindarajan M 2016. Green synthesis of silver, gold and silver/gold bimetallic nanoparticles using the *Gloriosa superba* leaf extract and their antibacterial and antibiofilm activities. Microb. Pathog. 101: 1–11.

Hatipoğlu, A. 2021. *Green synthesis of silver nanoparticles using Abelmoschus esculentus leaf and antimicrobial effects on some food pathogens*. ACU J. For. Fac. 2(2): 239–246.

Hemmati S, Rashtiani A, Zangeneh MM, Mohammadi P, Zangeneh A, Veisi H 2019. Green synthesis and characterization of silver nanoparticles using *Fritillaria* flower extract and their antibacterial activity against some human pathogens. Polyhedron 158: 8–14.

Jebril S, Khanfir Ben Jenana R, Dridi C 2020. Green synthesis of silver nanoparticles using Melia azedarach leaf extract and their antifungal activities: In vitro and in vivo. Mater. Chem. Phys. 248: 122898.

Kawarty, A.M.A. ; Behçet, L., Çakılcıoglu, U. (2020). An ethnobotanical survey of medicinal plants in Ballakayati (Erbil, North Iraq). Turk J Botany 44(3), 345–357.

Keser S, Keser F, Kaygili O, Tekin S, Turkoglu I, Demir E, Turkoglu S, Karatepe M, Sandal S, Kirbag S 2017. Phytochemical Compounds and Biological Activities of *Celtis tournefortii* Fruits . Anal. Chem. Lett. 7(3): 344–355.

Keskin C, Atalar MN, Baran MF, Baran A 2021. Environmentally Friendly Rapid Synthesis of Gold Nanoparticles from *Artemisia absinthium* Plant Extract and Application of Antimicrobial Activities. J. Inst. Sci. Tech. 11(1): 365-375.

Khalil, I., Yehye, W. A., Etxeberria, A. E., Alhadi, A. A., Dezfooli, S. M., Julkapli, N. B. M., Basirun, W. J., Seyfoddin, A (2019). Nanoantioxidants: Recent Trends in Antioxidant Delivery Applications. Antioxidants, 9(1): 24.

Khan AU, Yuan Q, Khan ZUH, Ahmad A, Khan FU, Tahir K, Shakeel M, Ullah S 2018. An eco-benign synthesis of AgNPs using aqueous extract of Longan fruit peel: Antiproliferative response against human breast cancer cell line MCF-7, antioxidant and photocatalytic deprivation of methylene blue. J. Photochem. Photobiol. B Biol. 183: 367–373.

Krishnaraj C, Jagan EG, Rajasekar S, Selvakumar P, Kalaichelvan PT, Mohan N 2010. Synthesis of silver nanoparticles using *Acalypha indica* leaf extracts and its antibacterial activity against water borne pathogens. Colloids Surf. B: Biointerfaces. 76(1): 50–56.

Kumar, R., Ghoshal, G. Jain A and GM 2017. Rapid Green Synthesis of Silver Nanoparticles (AgNPs) Using (*Prunus persica*) Plants extract: Exploring its Antimicrobial and Catalytic Activities. J. Nanomed. Nanotechnol. 8(4): 1–8.

Kumar B, Smita K, Cumbal L, Debut A 2015. Green synthesis of silver nanoparticles using *Andean blackberry* fruit extract. Saudi J. Biol. Sci. 24(1): 45–50.

Kumar V, Gundampati RK, Singh DK, Bano D, Jagannadham M V., Hasan SH 2016. Photoinduced green synthesis of silver nanoparticles with highly effective antibacterial and hydrogen peroxide sensing properties. J. Photochem. Photobiol. B Biol. 162: 374–385.

Kumar V, Singh S, Srivastava B, Bhadouria R 2019. Journal of Environmental Chemical Engineering Green synthesis of silver nanoparticles using leaf extract of *Holoptelea integrifolia* and preliminary investigation of its antioxidant , anti- in fl ammatory , antidiabetic and antibacterial activities. J. Environ. Chem. Eng. 7(3): 103094.

Luna C, Chávez VHG, Barriga-castro ED, Nú NO, Mendoza-reséndez R 2015. Biosynthesis of Silver Fine Particles and Particles Decorated with Nanoparticles Using the Extract of *Illicium verum* (Star Anise) Seeds. Spectrochim. ACTA PART A Mol. Biomol. Spectrosc. 141: 45–50.

Mohammadi F, Yousefi M, Ghahremanzadeh R 2019. Green Synthesis , Characterization and Antimicrobial Activity of Silver Nanoparticles (AgNPs) Using Leaves and Stems Extract of Some Plants. Adv. J. Chem. A 2(4): 266–275.

Mohmed A, Hassan S, Fouda A, Elgamal M, Salem S 2017. Extracellular Biosynthesis of Silver Nanoparticles Using *Aspergillus* sp. and Evaluation of their Antibacterial and Cytotoxicity. J. Appl. Life Sci. Int. 11(2): 1–12.

Morais M, Teixeira AL, Dias F, Machado V, Medeiros R, Prior JAV 2020. Cytotoxic Effect of Silver Nanoparticles Synthesized by Green Methods in Cancer. J. Med. Chem. 63(23): 14308–14335.

Narayan S, Dipak S 2015. Green synthesis of silver nanoparticles using fresh water green alga Pithophora oedogonia (Mont.) Wittrock and evaluation of their antibacterial activity. Appl. Nanosci. 5: 703–709.

Oliveira AC de J, Araújo AR de, Quelemes PV, Nadvorny D, Soares-Sobrinho JL, Leite JRS de A, da Silva-Filho EC, Silva DA da 2019. Solvent-free production of phthalated cashew gum for green synthesis of antimicrobial silver nanoparticles. Carbohydr. Polym. 213: 176–183.

Othman AM, Elsayed MA, Elshafei AM, Hassan MM 2017. Journal of Genetic Engineering and Biotechnology Application of response surface methodology to optimize the extracellular fungal mediated nanosilver green synthesis. J. Genet. Eng. Biotechnol. 15(2): 497–504.

Pallela PNVK, Ummey S, Ruddaraju LK, Pammi SVN, Yoon SG 2018. Ultra Small, mono dispersed green synthesized silver nanoparticles using

aqueous extract of *Sida cordifolia* plant and investigation of antibacterial activity. Microb. Pathog. 124: 63–69.

Pandiyan N, Murugesan B, Arumugam M, Sonamuthu J, Samayanan S, Mahalingam S 2019. Ionic liquid-A greener templating agent with Justicia adhatoda plant extract assisted green synthesis of morphologically improved Ag-Au/ZnO nanostructure and it's antibacterial and anticancer activities. J. Photochem. Photobiol. B Biol. 198: 111559.

Patil MP, Singh RD, Koli PB, Patil KT, Jagdale BS, Tipare AR, Kim G-D 2018. Antibacterial potential of silver nanoparticles synthesized using *Madhuca longifolia* flower extract as a green resource. Microb. Pathog. 121: 184–189.

Patra JK, Das G, Baek KH 2016. Phyto-mediated biosynthesis of silver nanoparticles using the rind extract of watermelon (*Citrullus lanatus*) under photo-catalyzed condition and investigation of its antibacterial, anticandidal and antioxidant efficacy. J. Photochem. Photobiol. B Biol. 161: 200–210.

Pugazhendhi S, Palanisamy PK, Jayavel R 2018. Synthesis of highly stable silver nanoparticles through a novel green method using Mirabillis jalapa for antibacterial, nonlinear optical applications. Opt. Mater. (Amst). 79: 457–463.

Rani P, Kumar V, Pal P, Singh A, Zhang W 2020. Highly stable AgNPs prepared via a novel green approach for catalytic and photocatalytic removal of biological and non-biological pollutants. Environ. Int. 143: 105924.

Rauf A, Ahmad T, Khan A, Maryam, Uddin G, Ahmad B, Mabkhot YN, Bawazeer S, Riaz N, Malikovna BK 2021. Green synthesis and biomedicinal applications of silver and gold nanoparticles functionalized with methanolic extract of *Mentha longifolia*. Artif. Cells, Nanomedicine Biotechnol. 49(1): 194–203.

Remya RR, Rajasree SRR, Aranganathan L, Suman TY 2015. An investigation on cytotoxic effect of bioactive AgNPs synthesized using Cassia fistula flower extract on breast cancer cell MCF-7. Biotechnol. Reports 8: 110–115.

Rolim WR, Pelegrino MT, de Araújo Lima B, Ferraz LS, Costa FN, Bernardes JS, Rodigues T, Brocchi M, Seabra AB seabra 2019. Green tea extract mediated biogenic synthesis of silver nanoparticles: Characterization, cytotoxicity evaluation and antibacterial activity. Appl. Surf. Sci. 463: 66–74.

Sarkar MK, Vadivel V, Charan Raja MR, Mahapatra SK 2018. Potential anti-proliferative activity of AgNPs synthesized using *M. longifolia* in 4T1 cell line through ROS generation and cell membrane damage. J. Photochem. Photobiol. B Biol. 186: 160–168.

Satpathy S, Patra A, Ahirwar B, Delwar Hussain M 2018. Antioxidant and anticancer activities of green synthesized silver nanoparticles using aqueous extract of tubers of *Pueraria tuberosa*. Artif. Cells, Nanomedicine Biotechnol. 46(3): 71–85.

Shao Y, Wu C, Wu T, Yuan C, Chen S, Ding T, Ye X, Hu Y 2018. Green synthesis of sodium alginate-silver nanoparticles and their antibacterial activity. Int. J. Biol. Macromol. 111: 1281–1292.

Singh A, Sharma B, Deswal R 2018. Green silver nanoparticles from novel Brassicaceae cultivars with enhanced antimicrobial potential than earlier reported Brassicaceae members. J. Trace Elem. Med. Biol. 47: 1–11.

Swamy MK, Akhtar MS, Mohanty SK, Sinniah UR 2015. Synthesis and characterization of silver nanoparticles using fruit extract of *Momordica cymbalaria* and assessment of their in vitro antimicrobial, antioxidant and cytotoxicity activities. Spectrochim. Acta - Part A Mol. Biomol. Spectrosc. 151: 939–944.

Thomas B, Vithiya BSM, Prasad TAA, Mohamed SB, Magdalane CM, Kaviyarasu K, Maaza M 2018. Antioxidant and Photocatalytic Activity of Aqueous Leaf Extract Mediated Green Synthesis of Silver Nanoparticles Using *Passiflora edulis f. flavicarpa*. J. Nanosci. Nanotechnol. 19(5): 2640–2648.

Ural E 2001.Endemic and medicinal plants in Gap region, Turkey Environment Foundation, 143, 63–64.

Vastrad J 2016. Green Synthesis and Characterization of Silver Nanoparticles Using Leaf Extract of *Tridax procumbens*. Asian J. Pharm. Res. 7(2): 44–48.

Velmurugan P, Anbalagan K, Manosathyadevan M, Lee KJ, Cho, MinJung-Hee Park, Sae-Gang Oh K-SB, Oh B-T, Lee SM 2014. Green synthesis of silver and gold nanoparticles using *Zingiber officinale* root extract and antibacterial activity of silver nanoparticles against food pathogens. Bioprocess Biosyst. Eng. 37(10): 1935–1943.

Wongpreecha J, Polpanich D, Suteewong T, Kaewsaneha C, Tangboriboonrat P 2018. One-pot, large-scale green synthesis of silver nanoparticles-chitosan with enhanced antibacterial activity and low cytotoxicity. Carbohydr. Polym. 199: 641–648.

Yıldırım I, Uğur Y, Kutlu T 2017. Investigation of Antioxidant Activity and Phytochemical Compositions of *Celtis tournefortii*. Free Radicals Antioxidants 7(2): 160–165.

Zein R, Alghoraibi I, Soukkarieh C, Salman A, Alahmad A 2020. *In-vitro* anticancer activity against Caco-2 cell line of colloidal nano silver synthesized using aqueous extract of *Eucalyptus camaldulensis* leaves. Heliyon 6(8): e04594.